Vapor−Liquid Equilibria of Ammonia + Water + Potassium Hydroxide and Ammonia + Water + Sodium Hydroxide Solutions at Temperatures from (293.15 to 353.15) K

Daniel Salavera, Shrirang K. Chaudhari,† Xavier Esteve, and Alberto Coronas*

Center of Technological Innovation CREVER, Universitat Rovira i Virgili, Autovía de Salou s/n, 43006 Tarragona, Spain

Vapor−liquid equilibria of ammonia + water + potassium hydroxide and ammonia + water + sodium hydroxide systems were measured by a static method from (293.15 to 353.15) K. The experimental vapor pressure data have been correlated with temperature and mass percent concentration using an analytical polynomial equation.

Introduction

Interest in absorption refrigeration systems driven by waste heat as an alternative to conventional power-driven systems has increased because of current energy and environmental issues. The working fluids commercially used are water + lithium bromide and ammonia + water. Nevertheless, these fluids have some disadvantages. Chillers using water + lithium bromide operate under high-vacuum conditions, and for this reason, they are voluminous and require air removal systems. In addition, they do not operate below an evaporation temperature of 4 °C and suffer crystallization and corrosion problems. They also require cooling water from a water-cooling tower for heat dissipation. However, the ammonia + water system requires rectification of the refrigerant vapor, operates at high pressure, and therefore requires resistant and heavy components. However, this system can be air-cooled and can operate at temperatures below 0 °C.

At the beginning of the 1990s, Reiner and Zaltash[1−3] studied the use of salts in ammonia + water systems in order to identify those that would allow a reduction of the partial pressure of water in the dissolution. The result showed that the addition of LiBr, LiCl, and $LiNO_3$ increased the boiling temperature of the ammonia + water system, whereas the addition of LiOH and KOH decreased it. In this way, the hydroxides favor ammonia separation due to the salting out effect, which will reduce the rectification load in absorption systems activated by low-temperature sources (less than 353.15 K). Balamaru et al.[4] have suggested the addition of sodium hydroxide to the ammonia + water system for the use of low-temperature heat sources. They simulated an absorption refrigeration cycle using the commercial process tool Aspen Plus and concluded that the addition of alkaline hydroxide increases the coefficient of performance and cooling capacity. Thermodynamic properties of the ternary system, especially vapor−liquid equilibria, are needed for the design of absorption heat pump systems. The literature for the ammonia + water + hydroxide system is scarce. Brass et al.[5] have measured vapor−liquid equilibria in the systems ammonia + water + sodium hydroxide and ammonia + water + potassium hydroxide at 303.15 K and 318.15 K and pressures between (0.1 and 1.3) MPa. Sing et al.[6] have measured the solubility of ammonia in aqueous NaOH solutions in the temperature range of (313.15 to 393.16) K. Solutions with (30 to 40) mass % ammonia are used in single-effect absorption cycles. In the present work, vapor−liquid equilibria for the binary ammonia + water system were measured by a static method in the temperature range of (293.15 to 353.15) K in 10 K steps for (10, 20, 30, 35, and 40) mass % ammonia concentrations to check the performance of the apparatus and experimental procedure. The measurements were repeated for the same ammonia concentrations and temperatures with potassium and sodium hydroxide concentrations (no salt basis) from (4 to 20) mass % in 4% steps.

To calculate the liquid composition at equilibrium from the total initial composition and the experimental pressure and temperature data, the Barker[7] method was applied to the ammonia water system, and the extension of the Barker[8] method was applied to ternary systems. The equilibrium data were correlated with an analytical equation used by Cacciola et al.[9] The calculated pressures using the analytical polynomial equation were compared with the experimental and available literature data.

Experimental Section

Materials. Ammonia (Carburos Metálicos, 99.98%), potassium hydroxide (Aldrich 99.99%, semiconductor-grade pellets), and sodium hydroxide (Aldrich 99.998% pellets) were used without further purification. All solutions were prepared using Millipore water (resistivity lower than 18.2 MΩ).

Equipment and Procedures. The vapor−liquid equilibria of ammonia + water + potassium hydroxide and ammonia + water + sodium hydroxide systems were measured by a static method. The apparatus has been described previously.[10] It consisted of an equilibrium cell, a differential pressure null transducer (DPT) (Ruska model 2439-702), a precise pressure controller (Ruska model 3891-801), and two Haake proportional temperature controllers

* To whom all the correspondence should be addressed. E-mail: acoronas@crever.urv.es. Fax: +34-977-542272.
† On sabbatical leave from the National Chemical Laboratory, Pune 411008, India.

10.1021/je049708+ CCC: $30.25
Published on Web 02/22/2005

(a Haake F6 unit for heating and a Haake EK90 immersion cooler for cooling) for a double-walled thermostated bath of 25 L capacity filled with water. The temperature in the bath was controlled to better than ±0.01 K and measured using a digital precision thermometer (Anton Paar MKT 100). Two cells for high-pressure measurements were made of stainless steel and had volumes of 149 cm^3 and 193 cm^3. The pressure was measured by two digital pressure gauges (Ruska model 6222 for pressures up to 130 kPa and up to 1 MPa and Ruska model 6220-750 for pressure up to 5 MPa). The pressure uncertainties were ±0.05 kPa for pressures lower than 130 kPa, ±0.3 kPa up to 1 MPa, and ±0.6 kPa for higher pressures. The components were weighed on a Mettler balance (Mettler Toledo PR2003DR) with a precision of $\pm 10^{-3}$ g.

The experimental procedure for vapor−liquid equilibria measurements is similar to that described in previous work.[10−13] The procedure to charge the equilibrium cell with ammonia + water is the same as that described by Coronas et al.[13] To prepare the ternary solutions, we charged in the cell with an aqueous hydroxide solution of known composition. Then, it was degassed by several freezing, vaccum extraction, and thawing cycles, and a weighed quantity of ammonia was introduced through an auxiliary cell. By weighing the auxiliary vessel before and after each charging, the mass of ammonia added was obtained. Potassium hydroxide pellets contained some residual water. The exact potassium hydroxide concentration was found by titration with hydrochloric acid using an Orion 960 authoterm system.

The calculation procedure for finding the equilibrium composition from the initial composition of the sample and the measured vapor pressure and temperature for ammonia + water was the same as that described by Herraiz et al.[11] A Redlich−Kister polynomial equation of degree 4 for the excess Gibbs free energy of the liquid phase was adopted, and the coefficients were obtained by fitting the P, x data at each temperature. To calculate the equilibrium composition of the ammonia + water + potassium hydroxide and ammonia + water + sodium hydroxide systems, we applied an extension of Barker's method to the ternary system, as suggested by Fonseca and Lobo.[8] In this approach, the following equation for the excess Gibbs free energy of the liquid phase was used.

$$\frac{G^E}{RT} = \sum_{ij} x_i x_j [A_{ij} + B_{ij}(x_i - x_j) + C_{ij}(x_i - x_j)^2] + x_1 x_2 x_3 (c_0 - c_1 x_1 - c_2 x_2) \quad (1)$$

The parameters of this equation were obtained by fitting P and x data at each temperature. The fit was made using a Marquardt nonlinear regression program minimizing the objective function

$$\mathrm{OF} = \sum_1^N \left[\frac{(P_i^{\mathrm{calcd}} - P_i^{\mathrm{exptl}})}{P_i^{\mathrm{exptl}}} \right]^2 \quad (2)$$

where N is the number of experimental points for a temperature.

The vapor-phase nonideality was modeled using the virial equation of state truncated after the second virial coefficient. The pure-component virial coefficients and the mixed second virial coefficient used were from Rumpf and Maurer.[14] We used only second virial and mixed virial coefficients for ammonia and water because in the vapor phase only these two components are present. The critical properties and the equations used for the vapor pressure and density of pure water were those of Saul and Wagner.[15] For the density of pure ammonia, the equation proposed by Haar and Gallagher[16] was used, and for the vapor pressure of pure ammonia, the equation given by Perry and Green[17] was used.

Table 1. Experimental Vapor Pressure Data for NH_3 + H_2O

$w$$NH_3$/mass %	P/kPa	$w$$NH_3$/mass %	P/kPa
293.15 K		333.15 K	
9.997	12.1	9.989	72.6
20.024	30.7	19.946	160.2
30.023	71.8	29.946	312.0
35.114	106.0	34.990	429.3
39.930	148.8	39.818	564.3
303.15 K		343.15 K	
9.996	19.8	9.987	101.6
20.010	50.5	19.921	223.7
30.008	112.9	29.925	423.1
35.093	156.3	34.956	574.0
39.910	216.2	39.789	743.5
313.15 K		353.15 K	
9.994	31.9	9.982	144.2
19.993	76.6	19.869	309.0
29.991	161.4	29.879	568.0
35.064	224.4	34.887	751.8
39.883	304.3	39.733	961.2
323.15 K			
9.992	48.3		
19.972	112.2		
29.971	226.0		
35.030	313.9		
39.853	419.0		

Table 2. Coefficients of Equation 3 for the NH_3 + H_2O System

coefficient	value	coefficient	value
A_0	1.658×10^1	B_0	-4.384×10^3
A_1	6.832×10^{-2}	B_1	1.277×10^1
A_2	-3.472×10^{-3}	B_2	8.180×10^{-1}
A_3	3.617×10^{-5}	B_3	-9.950×10^{-3}

Results and Correlations

To check the experimental and data-reduction procedure, we measured the vapor−liquid equilibria of the ammonia + water binary system from (293.15 to 353.15) K. The equilibrium data are shown in Table 1. The vapor-pressure data have been correlated with the following analytical polynomial equation similar to that proposed by Cacciola et al.[9] but changing from the decimal logarithm to the natural logarithm:

$$\ln(p/\mathrm{kPa}) = A_0 + A_1 m_1 + A_2 m_1^2 + A_3 m_1^3 + \frac{B_0 + B_1 m_1 + B_2 m_1^2 + B_3 m_1^3}{T/\mathrm{K}} \quad (3)$$

where m_1 is the ammonia mass percentage concentration and coefficients A_0, A_1, A_2, A_3, B_0, B_1, B_2, and B_3 are listed in Table 2. The root-mean-square relative deviation (rmsd) of the fit is 2%. The rmsd is defined by

$$\mathrm{rmsd} = 100 \left\{ \frac{1}{N} \sum_i \left(\frac{X_e - X_c}{X_e} \right)_i^2 \right\}^{1/2} \quad (4)$$

where N, X_e, and X_c are the number of data points and the experimental and calculated values, respectively. Our vapor−liquid equilibria data were compared with the best

Table 3. Experimental Vapor Pressure Data for NH_3 + H_2O + KOH

wNH$_3$	wKOH	P	wNH$_3$	wKOH	P	wNH$_3$	wKOH	P	wNH$_3$	wKOH	P
% mass	% mass	kPa	% mass	% mass	kPa	% mass	% mass	kPa	% mass	% mass	kPa
		T = 293.15 K						T = 333.15 K			
10.063	4.047	16.0	34.368	12.195	170.6	10.051	4.047	121.0	33.883	12.291	832.8
19.985	3.941	39.7	39.218	12.072	224.7	19.886	3.947	260.0	38.838	12.152	1058.0
30.480	3.966	94.5	9.880	16.082	25.5	30.318	3.976	517.0	9.868	16.085	176.5
34.838	3.980	126.4	19.899	15.947	70.0	34.446	4.005	650.2	19.867	15.955	408.8
39.733	3.920	172.3	29.907	15.975	147.1	39.419	3.941	840.9	29.692	16.029	752.8
10.034	8.031	18.5	34.848	15.988	196.0	10.033	8.032	136.6	34.300	16.133	940.0
19.858	8.022	47.7	38.965	16.047	253.6	19.746	8.035	299.3	38.556	16.161	1169.8
30.288	7.980	112.1	9.822	19.926	29.5	30.110	8.002	587.1	9.809	19.930	199.9
34.597	8.194	149.0	19.774	19.999	81.5	34.155	8.253	744.8	19.744	20.008	456.0
39.474	7.990	201.0	29.711	20.034	171.9	39.129	8.037	944.5	29.482	20.106	843.1
9.974	12.012	22.5	34.603	20.152	223.0	9.974	12.012	153.2	34.009	20.351	1044.1
19.732	12.019	58.3	38.715	19.982	285.0	19.604	12.041	353.6	38.279	20.134	1285.1
30.098	11.988	126.7				29.901	12.025	665.8			
		T = 303.15 K						T = 343.15 K			
10.062	4.047	25.5	34.311	12.207	247.0	10.048	4.048	169.0	33.730	12.322	1071.0
19.974	3.942	61.0	39.168	12.083	325.7	19.852	3.949	352.7	38.721	12.177	1357.0
30.460	3.967	139.8	9.879	16.082	40.2	30.266	3.979	680.6	9.864	16.086	241.0
34.789	3.983	184.7	19.895	15.948	105.5	34.320	4.014	845.4	19.859	15.957	542.8
39.692	3.923	249.0	29.883	15.982	215.7	39.324	3.948	1081.0	29.627	16.045	976.0
10.034	8.031	29.9	34.787	16.007	283.9	10.034	8.032	189.3	34.129	16.179	1201.5
19.846	8.024	72.6	38.916	16.063	365.3	19.709	8.040	403.0	38.434	16.196	1489.0
30.267	7.982	161.2	9.821	19.926	47.3	30.054	8.009	768.0	9.806	19.931	271.0
34.543	8.202	216.0	19.771	20.001	122.3	34.016	8.272	960.4	19.736	20.011	613.5
39.431	7.996	284.2	29.690	20.043	249.2	39.026	8.052	1210.0	29.413	20.128	1086.0
9.974	12.012	34.0	34.546	20.179	324.0	9.975	12.011	211.2	33.806	20.419	1350.5
19.719	12.021	87.6	38.673	20.003	406.6	19.562	12.049	470.5	38.149	20.179	1630.0
30.075	11.993	186.9				29.841	12.036	865.8			
		T = 313.15 K						T = 353.15 K			
10.060	4.047	39.4	34.230	12.222	346.0	10.011	3.989	166.0	29.986	15.986	1069.0
19.959	3.943	91.3	39.103	12.096	452.9	9.971	8.081	199.6	29.991	19.977	1225.2
30.434	3.969	200.0	9.876	16.083	60.6	9.934	12.005	235.0	34.782	3.917	865.2
34.727	3.987	261.6	19.889	15.950	153.3	9.976	15.999	268.0	34.776	8.047	1010.0
39.640	3.926	350.0	29.844	15.991	306.0	9.976	20.008	312.6	34.709	12.060	1178.0
10.033	8.032	45.6	34.690	16.030	396.0	19.660	4.152	361.6	34.645	16.113	1343.6
19.828	8.026	107.4	38.842	16.081	506.2	19.550	8.063	425.1	34.577	20.233	1524.0
30.239	7.986	229.3	9.818	19.927	70.7	19.501	12.080	500.0	39.697	3.928	1086.0
34.469	8.211	307.0	19.764	20.002	177.4	19.591	16.071	585.7	39.644	8.075	1260.0
39.373	8.003	397.3	29.645	20.055	348.3	19.268	20.135	686.0	39.949	11.966	1460.0
9.973	12.012	51.7	34.425	20.212	455.0	29.928	3.999	669.5	39.447	16.185	1661.0
19.698	12.025	129.3	38.586	20.027	559.4	30.600	8.015	805.4	39.510	20.057	1829.0
30.041	11.999	267.0				30.125	12.113	931.3			
		T = 323.15 K									
10.055	4.047	85.4	34.019	12.264	635.2						
19.915	3.945	187.7	38.939	12.131	815.0						
30.363	3.973	385.6	9.871	16.084	126.9						
34.556	3.998	490.8	19.875	15.953	303.0						
39.504	3.936	641.5	29.752	16.014	569.5						
10.033	8.032	96.6	34.454	16.093	720.4						
19.779	8.032	218.2	38.667	16.131	904.0						
30.159	7.995	439.9	9.813	19.929	144.8						
34.278	8.237	566.6	19.751	20.006	344.7						
39.223	8.024	723.8	29.546	20.086	642.5						
9.974	12.012	109.2	34.181	20.295	800.0						
19.642	12.035	258.6	38.400	20.093	994.5						
29.954	12.015	503.9									

available data of Smolen et al.[18] and Tillner-Roth and Friend,[19] (calculated from eq 3). The rmsd values between their experimental data and our calculated data were 1.38% and 1.17%, respectively.

The experimental vapor-pressure data and compositions in mass percent of ammonia and potassium or sodium hydroxide are listed in Tables 3 and 4, respectively. These results also were correlated in a similar form with the temperature and mass percent of ammonia and potassium or sodium hydroxide dependence using the same analytical polynomial equation proposed by Cacciola et al.[9] (eq 3), but in this case, coefficients A_0, A_1, A_2, A_3, B_0, B_1, B_2, and B_3 are polynomial functions of the potassium (or sodium) hydroxide mass percent concentration.

$$A_i = \sum_{j=0}^{2} a_{ij} m_2^j \qquad B_i = \sum_{j=0}^{2} b_{ij} m_2^j \qquad \text{with } i = 0-3 \quad (5)$$

Coefficients a_{ij} and b_{ij} are listed in Tables 5 and 6 for the two systems studied. Compositions m_1 and m_2 (on a salt-free solution basis) are defined by

$$m_1 = \frac{\text{mass}_{NH_3}}{\text{mass}_{NH_3} + \text{mass}_{H_2O}} \cdot 100$$

$$m_2 = \frac{\text{mass}_{XOH}}{\text{mass}_{NH_3} + \text{mass}_{H_2O}} \cdot 100 \quad (6)$$

Table 4. Experimental Vapor Pressure Data for NH_3 + H_2O + NaOH

wNH$_3$	wNaOH	P	wNH$_3$	wNaOH	P	wNH$_3$	wNaOH	P	wNH$_3$	wNaOH	P
% mass	% mass	kPa	% mass	% mass	kPa	% mass	% mass	kPa	% mass	% mass	kPa
		T = 293.15 K						T= 333.15 K			
10.073	3.986	13.5	30.004	15.982	171.0	10.042	3.987	82.0	29.985	15.986	629.6
9.997	8.078	18.8	30.002	19.973	204.2	9.983	8.079	103.1	29.985	19.978	729.7
9.991	11.997	25.1	34.776	3.917	130.0	9.963	12.001	120.0	34.771	3.917	501.0
9.986	15.997	31.3	35.089	8.007	156.5	9.979	15.998	143.8	34.910	8.030	605.0
9.985	20.006	40.1	35.070	11.993	196.0	9.979	20.007	169.0	34.869	12.030	703.4
20.077	4.127	40.3	35.053	16.012	232.2	19.869	4.139	190.7	34.824	16.068	812.5
19.829	8.033	51.9	35.033	20.092	275.3	19.684	8.049	233.6	34.775	20.172	932.1
19.944	12.011	65.4	39.923	3.912	172.0	19.713	12.047	280.1	39.793	3.921	641.1
19.888	16.011	82.0	39.992	8.028	208.8	19.731	16.043	333.0	39.794	8.055	755.4
19.774	20.008	104.3	40.106	11.934	249.5	19.503	20.076	401.5	40.005	11.954	898.0
29.958	3.997	92.8	39.663	16.127	306.0	29.937	3.998	374.2	39.532	16.162	1013.5
30.723	8.000	118.4	39.861	19.941	358.3	30.652	8.009	463.0	39.658	20.008	1125.8
30.122	12.114	142.6				30.115	12.115	544.5			
		T = 303.15 K						T= 343.15 K			
10.068	3.986	22.6	29.999	15.983	243.2	10.030	3.988	120.0	29.985	15.987	828.1
9.994	8.078	30.3	29.997	19.975	289.0	9.979	8.080	145.0	29.987	19.978	953.2
9.985	11.997	39.3	34.774	3.917	188.0	9.955	12.003	172.0	34.774	3.917	663.0
9.984	15.997	47.8	35.056	8.012	230.1	9.979	15.998	198.1	34.855	8.038	785.5
9.984	20.006	57.6	35.034	11.999	277.8	9.979	20.007	230.1	34.803	12.044	919.7
20.043	4.129	61.7	35.012	16.022	326.0	19.787	4.145	265.0	34.753	16.089	1055.0
19.803	8.036	79.0	34.986	20.106	383.4	19.634	8.056	319.1	34.702	20.200	1195.5
19.903	12.017	98.0	39.899	3.914	247.0	19.640	12.062	378.4	39.749	3.924	843.0
19.860	16.016	120.6	39.955	8.033	299.2	19.685	16.056	446.0	39.729	8.064	985.0
19.728	20.019	149.6	40.086	11.938	358.1	19.438	20.102	522.4	39.979	11.960	1157.0
29.953	3.997	135.4	39.639	16.134	418.9	29.932	3.998	506.4	39.497	16.174	1306.4
30.709	8.002	172.9	39.828	19.951	472.0	30.630	8.012	617.0	39.599	20.031	1445.0
30.119	12.114	207.3				30.118	12.115	719.4			
		T= 313.15 K						T = 353.15 K			
10.061	3.986	37.0	29.994	15.984	342.4	10.011	3.989	166.0	29.986	15.986	1069.0
9.991	8.078	48.7	29.992	19.976	402.3	9.971	8.081	199.6	29.991	19.977	1225.2
9.978	11.998	60.0	34.772	3.917	261.4	9.934	12.005	235.0	34.782	3.917	865.2
9.983	15.997	71.2	35.018	8.016	320.9	9.976	15.999	268.0	34.776	8.047	1010.0
9.982	20.006	85.5	34.989	12.008	386.6	9.976	20.008	312.6	34.709	12.060	1178.0
19.999	4.132	92.2	34.959	16.035	454.2	19.660	4.152	361.6	34.645	16.113	1343.6
19.772	8.039	116.6	34.927	20.124	527.4	19.550	8.063	425.1	34.577	20.233	1524.0
19.854	12.025	142.3	39.869	3.916	348.0	19.501	12.080	500.0	39.697	3.928	1086.0
19.826	16.023	173.7	39.911	8.039	417.0	19.591	16.071	585.7	39.644	8.075	1260.0
19.668	20.034	213.4	40.062	11.943	498.7	19.268	20.135	686.0	39.949	11.966	1460.0
29.948	3.997	191.6	39.607	16.142	575.0	29.928	3.999	669.5	39.447	16.185	1661.0
30.693	8.004	245.3	39.780	19.967	644.5	30.600	8.015	805.4	39.510	20.057	1829.0
30.117	12.115	290.4				30.125	12.113	931.3			
		T= 323.15 K									
10.054	3.987	55.3	29.989	15.985	469.1						
9.988	8.079	71.7	29.988	19.978	547.5						
9.972	11.999	87.5	34.771	3.917	362.5						
9.981	15.998	102.6	34.972	8.022	441.6						
9.981	20.007	121.4	34.935	12.018	527.1						
19.944	4.135	134.4	34.897	16.050	615.2						
19.735	8.043	167.0	34.858	20.146	708.4						
19.794	12.035	202.7	39.834	3.918	477.7						
19.785	16.032	243.5	39.858	8.046	568.0						
19.597	20.053	295.8	40.035	11.948	676.8						
29.943	3.998	270.9	39.572	16.152	771.6						
30.675	8.006	340.6	39.723	19.986	861.7						
30.115	12.115	397.6									

Table 5. Coefficients of Equation 5 for the NH_3 + H_2O + KOH System

coefficient	value	coefficient	value
a_{00}	1.594×10^{1}	b_{00}	-4.106×10^{3}
a_{01}	1.303×10^{-1}	b_{01}	-5.351×10^{1}
a_{02}	-4.018×10^{-3}	b_{02}	1.878×10^{0}
a_{10}	6.296×10^{1}	b_{10}	1.991×10^{-1}
a_{11}	-7.283×10^{-3}	b_{11}	5.437×10^{0}
a_{12}	-7.633×10^{-5}	b_{12}	-4.441×10^{-2}
a_{20}	-1.865×10^{-3}	b_{20}	8.730×10^{-1}
a_{21}	-8.022×10^{-5}	b_{21}	-8.592×10^{-2}
a_{22}	2.029×10^{-5}	b_{22}	-4.331×10^{-3}
a_{30}	6.813×10^{-6}	b_{30}	-7.607×10^{-3}
a_{31}	4.713×10^{-6}	b_{31}	-2.839×10^{-4}
a_{32}	-4.085×10^{-7}	b_{32}	1.086×10^{-4}

Table 6. Coefficients of Equation 5 for the NH_3 + H_2O + NaOH System

coefficient	value	coefficient	value
a_{00}	1.724×10^{0}	b_{00}	-4.682×10^{2}
a_{01}	-2.368×10^{-1}	b_{01}	1.052×10^{0}
a_{02}	9.744×10^{-3}	b_{02}	-3.960×10^{0}
a_{10}	4.500×10^{-2}	b_{10}	2.480×10^{0}
a_{11}	5.399×10^{-3}	b_{11}	-2.779×10^{1}
a_{12}	-4.571×10^{-4}	b_{12}	2.282×10^{-1}
a_{20}	-4.469×10^{-3}	b_{20}	1.064×10^{0}
a_{21}	2.311×10^{-4}	b_{21}	-4.678×10^{-2}
a_{22}	3.082×10^{-7}	b_{22}	-2.752×10^{-3}
a_{30}	6.574×10^{-5}	b_{30}	-1.979×10^{-2}
a_{31}	-6.004×10^{-6}	b_{31}	1.705×10^{-3}
a_{32}	1.381×10^{-7}	b_{32}	-1.908×10^{-5}

where X represents K or Na. The root-mean-square relative deviation (rmsd) for the fit is 1.39% for ammonia + water + potassium hydroxide and 2.37% for ammonia + water + sodium hydroxide. In Figures 1 and 2, the experimental and calculated pressure from eqs 5 and 6 at 323.15 K for the two ternary systems are shown for comparison. Rela-

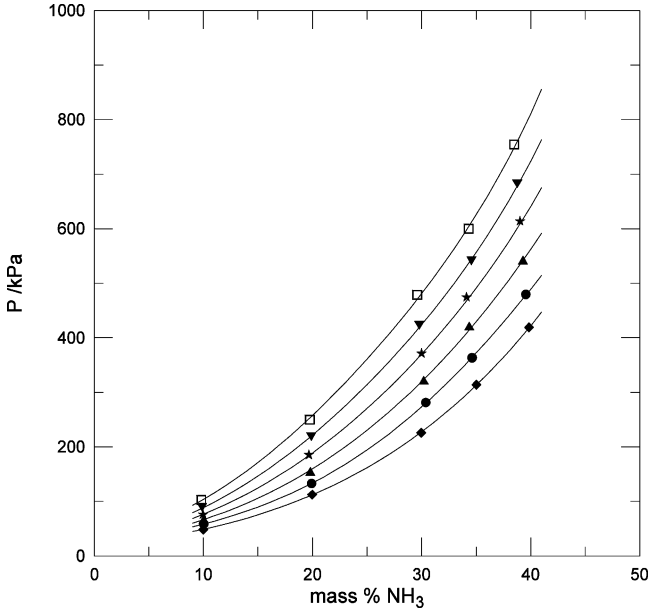

Figure 1. Total pressure of ammonia + water + potassium hydroxide solutions at 323.15 K: −, calculated pressure from eqs 3 and 5. Experimental results: ◆, 0 mass % KOH; ●, 4 mass % KOH; ▲, 8 mass % KOH; ★, 12 mass % KOH; ▼, 16 mass % KOH; □, 20 mass % KOH.

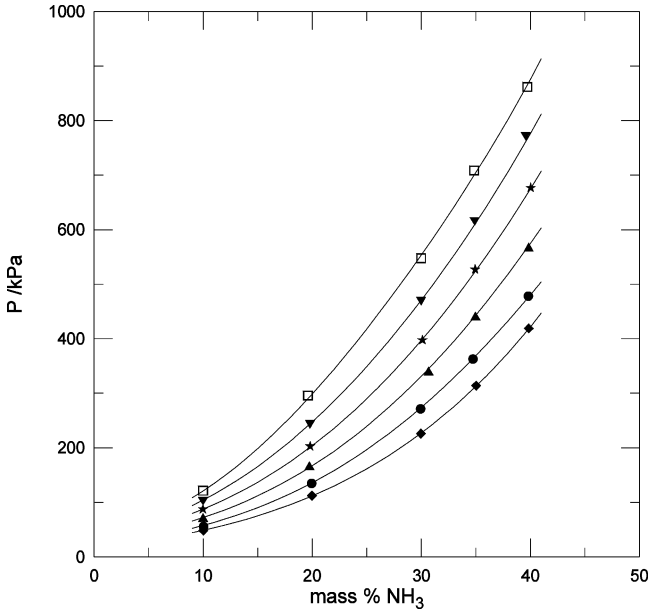

Figure 2. Total pressure of ammonia + water + sodium hydroxide solutions at 323.15 K: −, calculated pressure from eqs 3 and 5. Experimental results: ◆, 0 mass % NaOH; ●, 4 mass % NaOH; ▲, 8 mass % NaOH; ★, 12 mass % NaOH; ▼, 16 mass % NaOH; □, 20 mass % NaOH.

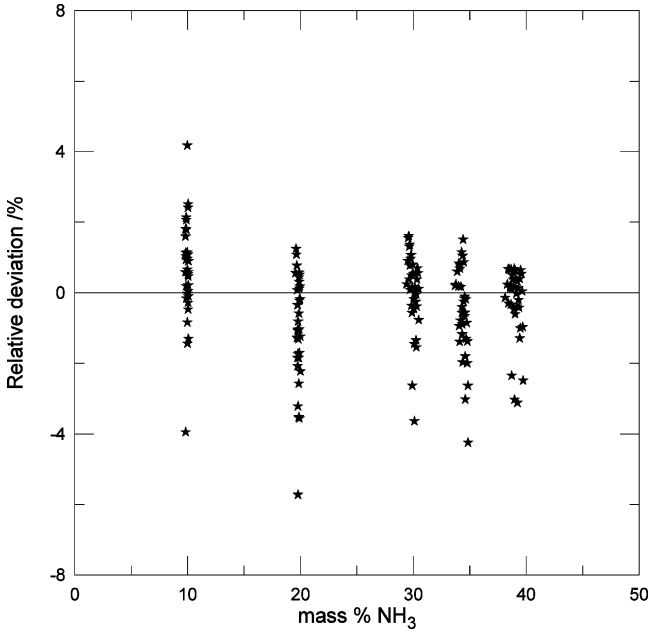

Figure 3. Relative deviation between the body of experimental and calculated vapor-pressure data for the NH_3 + H_2O + KOH system.

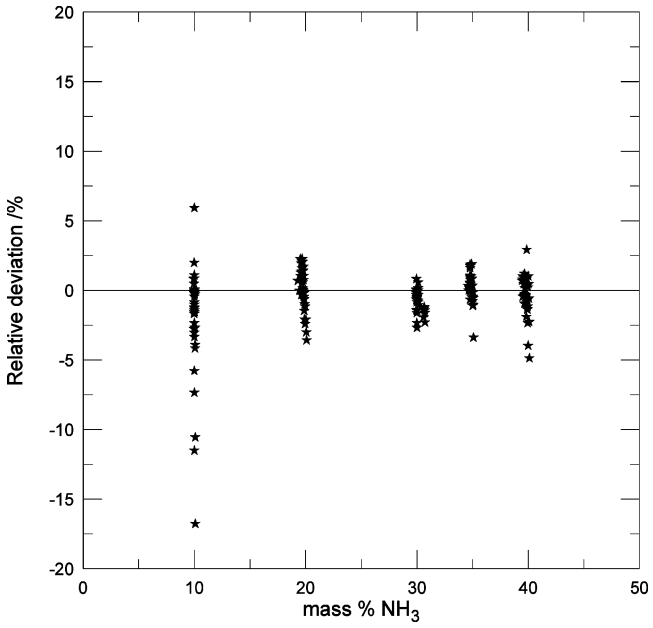

Figure 4. Relative deviation between the body of experimental and calculated vapor-pressure data for the NH_3 + H_2O + NaOH system.

tive deviations between the experimental and calculated data are shown in Figures 3 and 4 for ammonia + water + potassium hydroxide and ammonia + water + sodium hydroxide, respectively. In these Figures, it is seen that the maximum deviation are lower that 4% and 5%, respectively, but only for low concentrations of ammonia. For the ammonia + water + sodium hydroxide system, the deviations are larger (maximum deviation, −16.7%). Equations 5 and 6 were used to estimate the deviations between the experimental literature data and our calculated pressure for the ternary system. The rmsd between the calculated data and experimental data of Sing et al.[6] for ammonia + water + sodium hydroxide is 2.6% for the same range of temperature and mass percent concentration, whereas the rmsd for the Brass et al.[5] data is 8.0% for the same system and 4.8% for the ammonia + water + potassium hydroxide system. Brass et al.[5] observed phase separation at 303.15 K and 318.15 K at high concentration of ammonia. In the present study, for the concentration range studied, no phase separation was observed. Plots of ln P versus $-1000/T$ (Figures 5 and 6) show linear behavior, and the pressure increases with temperature and salt composition.

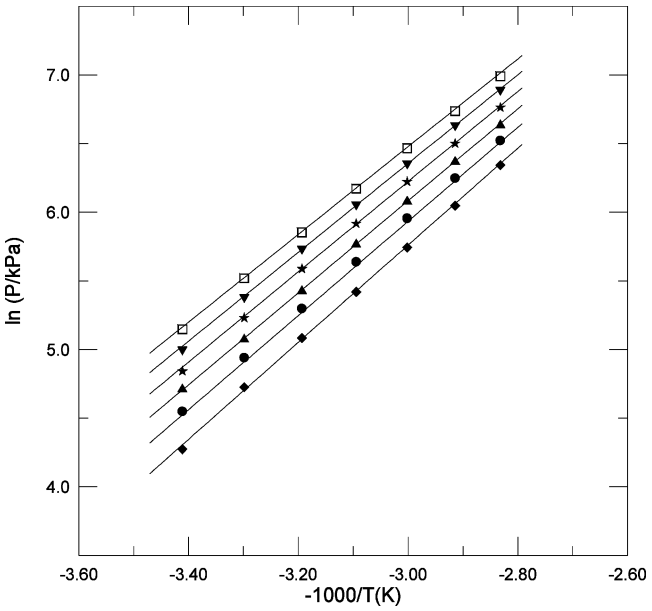

Figure 5. ln p of ammonia + water + potassium hydroxide solutions vs (−1000/T) at 30 mass % ammonia: −, calculated from eqs 3 and 5. Experimental results; ◆, 0 mass % KOH; ●, 4 mass % KOH; ▲, 8 mass % KOH; ★, 12 mass % KOH; ▼, 16 mass % KOH; □, 20 mass % KOH.

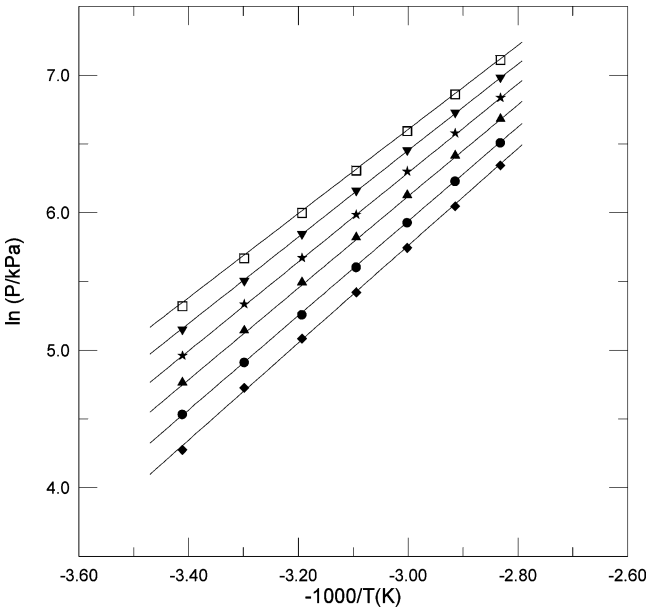

Figure 6. ln p of ammonia + water + sodium hydroxide solutions vs (−1000/T) at 30 mass % ammonia: −, calculated pressure from eqs 3 and 5. Experimental results: ◆, 0 mass % NaOH; ●, 4 mass % NaOH; ▲, 8 mass % NaOH; ★, 12 mass % NaOH; ▼, 16 mass % NaOH; □, 20 mass % NaOH.

Conclusions

The total pressure of ammonia + water + potassium hydroxide and ammonia + water + sodium hydroxide solutions was measured from (293.15 to 353.15) K in 10 K steps for (10 to 40) mass % ammonia concentrations and (0 to 20) mass % hydroxide concentrations. The data were fit by an analytical equation that was used to compare the calculated values with the experimental literature data.[5,6] The studied ternary systems are highly nonideal, and for that reason there is no other model available that fits all of the data well in the given concentration and temperature ranges. Fitting is for limited interpolations only.

Literature Cited

(1) Reiner, R. H.; Zaltash, A. Evaluation of ternary ammonia-water fluids for GAX and regenerative absorption cycles. Report ORNL/CF-91/263, 1991.
(2) Reiner, R. H.; Zaltash A. Corrosion Screening of potential fluids for ammonia water absorption cycles. Report ORNL/CF-92/41, 1992.
(3) Reiner, R. H.; Zaltash A. Densities and viscosities of ternary ammonia water fluids. ASME Winter Annual Meeting, 1993.
(4) Balamuru, V. G.; Ibrahim, O. M.; Barnett, S. M. Simulation of ternary ammonia−water-salt absorption refrigeration cycles. *Int. J. Refrig.* **2000**, *23*, 31−42.
(5) Brass, M.; Pritzel, T.; Schulte, E.; Keller, J. U. Measurements of Vapor-Liquid equilibria in the systems NH_3-H_2O-NaOH and NH_3-H_2O-KOH at temperatures of 303 and 318 K and pressures of 0.1 MPa<p<1.3 MPa. *Int. J. Thermophys.* **2000**, *21*, 883−898.
(6) Sing, R.; Rumpf, B.; Maurer, G. Solubility of Ammonia in Aqueous Solutions of Single Electrolytes Sodium Chloride, Sodium Nitrate, Sodium Acetate, and Sodium Hydroxide. *Ind. Eng. Chem. Res.* **1999**, *38*, 2098−2109.
(7) Barker, J. A. Determination of Activity Coefficients from Total Pressure Measurements. *Aust. J. Chem*, **1953**, *6*, 207−210.
(8) Fonseca, I. M. A.; Lobo, L. Q. Error analysis in Barker method. *Fluid Phase Equilib*. **1999**, *154*, 205−211.
(9) Cacciola, G.; Restuccia, G.; Aristov, Y. Vapor Pressure of (Potassium Hydroxide + Ammonia + Water) Solutions. *J. Chem. Eng. Data* **1995**, *40*, 267−270.
(10) Esteve, X.; Chaudhari, S. K.; Coronas, A. Vapor−Liquid Equilibria for Methanol + Tetraethylene Glycol Dimethyl Ether. *J. Chem. Eng. Data* **1995**, *40*, 1252−1256.
(11) Herraiz, J.; Shen, S.; Coronas, A. Vapor−Liquid Equilibria for Methanol + Polyethylene Glycol 250 Dimethyl Ether. *J. Chem. Eng. Data* **1998**, *43*, 191−195.
(12) Herraiz, J.; Olivé, F.; Zhu, S.; Shen, S.; Coronas, A. Thermophysical Properties of 2,2,2-Trifluoroethanol + Tetraethylene Glycol Dimethyl Ether. *J. Chem. Eng. Data* **1999**, *44*, 750−756.
(13) Coronas, A.; Mainar, A. M.; Patil, K. R.; Conesa, A.; Shen, S.; Zhu, S. Solubility of 1,1,1,2-Tetrafluoroethane in Triethylene Glycol Dimethyl Ether. *J. Chem. Eng. Data* **2002**, *47*, 56−58.
(14) Rumpf, B.; Maurer, G. Solubility of Ammonia in Aqueous Solutions of Sodium Sulfate, and Ammonium Sulfate at Temperatures from 333.15 K to 433.15 K and Pressures up to 3 MPa. *Ind. Eng. Chem. Res.* **1993**, *32*, 1780−1789.
(15) Saul, A.; Wagner, W. International equations for the saturation properties of ordinary water substance. *J. Phys. Chem. Ref. Data.* **1987**, *16*, 893−901.
(16) Haar, L.; Gallagher, J. S. Thermodynamic Properties of Ammonia. *J. Phys. Chem. Ref. Data.* **1978**, *7*, 635−792.
(17) Perry, R. H.; Green, D. W. *Perry's Chemical Enginneers Handbook*, 7th ed.; McGraw-Hill: New York, 1997.
(18) Smolen, T. M.; Manley, D. B.; Poling, B. E. Vapor−Liquid Equilibrium Data for the NH_3−H_2O System and Its Description with a Modified Cubic Equation of State. *J. Chem. Eng. Data*. **1991**, *36*, 202−208.
(19) Tillner-Roth, R.; Friend, D. G.; Survey and Assessment of Available Measurements on Thermodynamic Properties of the Mixture {Water+Ammonia}. *J. Phys. Chem. Ref. Data.* **1998**, *27*, 45−61.

Received for review August 12, 2004. Accepted January 17, 2005. This research project was financially supported by the Ministerio de Ciencia y Tecnología of Spain (DPI003-04752). Dr. S. K. Chaudhari thanks the Ministerio de Eduación y Ciencia (SAB2002-0050) of Spain for a fellowship.

JE049708+